Polish Journal of Microbiology
2020, Vol. 69, No 1, 39–48
https://doi.org/10.33073/pjm-2020-006

ORIGINAL PAPER

Impact of Hydrogen on the Transcriptome of *Sinorhizobium meliloti* 1021 Using RNA-sequencing Technology

RUIRUI LIU, LULU LI, ZHIYING LI and WEIWEI WANG*

The College of Life Sciences, Northwest University, Xi'an, P.R. China
Key Laboratory of Resource Biology and Biotechnology in Western China,
Northwest University, Xi'an, P.R. China

Submitted 29 August 2019, revised 11 January 2020, accepted 12 January 2020

Abstract

Hydrogen formed during nitrogen fixation in legumes can enter the surrounding soil and confer multiple benefits to crops. Here, we used *Sinorhizobium meliloti* 1021, whose genome was sequenced in 2001, as a model bacterium to study the relationship between the bacterium and legume. We investigated the effects of hydrogen on the gene expression in *S. meliloti* using RNA-sequencing technology. We identified 43 genes whose expression was altered by hydrogen treatment; among these, 39 were downregulated, and 4 were upregulated. These genes accounted for 1.5% of the total 2941 annotated genes of the *S. meliloti* genome. Gene ontology and pathway analyses revealed that the hydrogen-regulated genes were associated with catalytic activity and binding. Further, these genes were primarily involved in arginine, proline, and β-alanine metabolism. Real-time PCR revealed that the transcription levels of *SMc02983*, *cyoB*, *cyoC*, and *cyoD* were reduced after hydrogen treatment. These results provide a theoretical framework for exploring new metabolic pathways of *S. meliloti*.

Key words: *Sinorhizobium meliloti*, hydrogen, RNA-Seq, proline, oxidative phosphorylation

Introduction

Many microorganisms associated with plants are active in the rhizosphere; those that promote plant growth, control diseases, and increase crop yield are collectively referred to as plant growth-promoting rhizobacteria (PGPR). *Sinorhizobium meliloti* is an important PGPR that carries out biological nitrogen fixation through symbiosis with its hosts. This symbiosis has several benefits in agriculture, such as reducing the need for adding nitrogen fertilizers to the soil and improving crop tolerance (Wang et al. 2016). In many legume nodules, H_2 produced as a byproduct of N_2 fixation diffuses out of the nodules and is absorbed by the soil (Dong et al. 2001).

Previous studies have demonstrated that nitrogen fertilizers cannot completely replace the beneficial rotation effect of legumes. The 75% increase in the yield of soybean cannot be explained by existing theories (Heaterman et al. 1986). The nodules on legumes release large amounts of H_2 during nitrogen fixation. Approximately 1.5 mol of H_2 is produced for every unit of N_2 fixed. Soybeans with nitrogen-fixing capacity can produce approximately 5000 l of H_2 per hectare per day at peak growth and 2.4×10^5 l H_2 per hectare per the growing season. The production of H_2 requires 5–6% of the net energy produced during photosynthesis (Dong et al. 2003). From a metabolic point of view, the release of H_2 from the root is a waste of energy; however, neither long-term natural evolution nor manual screening strategies have successfully reduced this energy loss.

Most of the hydrogen released from legume nodules is absorbed by the soil (La Favre et al. 1983). A large amount of hydrogen is released during the nitrogen fixation process, but only a small amount is released into the atmosphere because of the actions of soil microorganisms that harvest the produced H_2 for energy. Kärst et al. (1987) demonstrated that hydrogen-utilizing bacteria could promote plant growth because they possess hydrogenase, a metal-containing protein that catalyzes the reduction of protons to produce hydrogen as an

* Corresponding author: W. Wang, The College of Life Sciences, Northwest University, Xi'an, P.R. China; Key Laboratory of Resource Biology and Biotechnology in Western China, Northwest University, Xi'an, P.R. China; **e-mail: wwwang@nwu.edu.cn**

end product of the electron transport chain (Kärst et al. 1987). The reversible reaction of catalytic protons to electron production is as follows: $2H^+ + 2e^- \leftrightarrow H_2$.

S. meliloti 1021 is a Gram-negative soil bacterium that can co-produce nitrogen in the nodules of legumes. *S. meliloti* 1021 fixes the gaseous-phase nitrogen into ammonia; consequently, the fixed nitrogen, in the form of ammonia or alanine, is supplied to the host plant, which in turn provides nutrients to the resident bacteria (Spaink 2000).

This study aimed to provide a new understanding of the role of hydrogen in the plant-rhizobacterium interaction and gain a better understanding of metabolic processes underlying these relationships using *S. meliloti* 1021 as a model bacterium. To this end, we conducted transcriptome analysis of *S. meliloti* 1021 using RNA-sequencing (RNA-Seq) technology to identify differentially expressed genes in the presence and absence of hydrogen.

Experimental

Materials and Methods

Bacteria. The strain is a model bacterial strain used to study the relationship between Rhizobium and legume (Barnett et al. 2001; Capela et al. 2001; Galibert et al. 2001). Single colonies were preserved in our laboratory and maintained on nutrient agar slants. Nutrient agar was prepared by dissolving 3 g beef extract, 5 g peptone, 5 g NaCl, and 15 g agar in 1000 ml distilled water (pH 7.2), followed by sterilization using an autoclave. The agar slants were stored at 4°C until use.

Hydrogen treatment. Ten milliliters of the prepared mineral salt medium was spread flat over the bottom of the glass culture flask and inoculated with *S. meliloti* 1021. This experiment was performed in triplicate. After the glass culture flask was sealed with a sterile rubber stopper, hydrogen (Wuhan Newradar Special Gas Company, Wuhan, Hubei Province, China) gas was injected into the flask from the sampler until uniformly distributed, and then the flask was placed horizontally on a shaker (80 rpm, 28°C). Hydrogen concentration was determined by gas chromatography at 13 000 ppm. In addition, the relative oxygen content was calculated to be 1.8% (Trace-1300; Thermo Fisher Scientific (Shanghai, China) Co., Ltd.) on a column (30 m × 0.32 mm × 30.0 μm) by setting the Thermal Conductivity Detector (TCD) temperature to 200°C and split ratio to 15:1. Air was provided to the control group. After incubation for 24, 48, and 72 h, the cells were washed with phosphate-buffered saline and centrifuged. The experiment was conducted with three biological replicates in each group.

Preparation and detection of RNA samples. Equal numbers of hydrogen-treated and control samples were combined to extract total RNA. The mRNA was fragmented, and the fragments were used as templates for reverse transcription to synthesize the first-strand cDNA using ProtoScript II Reverse Transcriptase (New England Biolabs, Ipswich, MA, USA), random primers, and actinomycin D. Second-strand cDNA was synthesized using Second Strand Synthesis Enzyme Mix (New England Biolabs). It was purified using AxyPrep Mag PCR Clean-up (Axygen) and treated with End Prep Enzyme Mix (Axygen) to repair both ends and add dA-tails in a single reaction. Following end-repair and adaptor ligation, RNA-seq data were obtained using a HiSeq instrument (Illumina, San Diego, CA, USA).

Data analysis. As the genome of *S. meliloti* 1021 has already been sequenced, DNA microarrays can be used to study the regulation of gene expression. Clean data from RNA-Seq were aligned to the *S. meliloti* 1021 reference genome using Bowtie2 (Langmesd et al. 2012). Significant differences between the hydrogen-treated and control groups were identified by setting the false discovery rate (FDR) *p*-value threshold at 0.05. The DESeq package based on the negative binomial distribution was used for this analysis. The open reading frames of the transcriptome data were annotated for taxonomic compositions and functions. We used the Kyoto Encyclopedia of Genes and Genomes (KEGG) database (Kanehisa et al. 2000) for the analysis of pathways associated with the differentially expressed genes. Moreover, the differentially expressed genes were subjected to the Gene Ontology (GO) enrichment for functional annotation, an internationally standardized gene function classification system that provides a dynamically updated vocabulary to fully describe the properties of genes and gene products in an organism (Li et al. 2015).

RT-qPCR and physiological research verification. For the specific genes *SMc02983*, *SMc01578*, *SMc01656*, *SMc02677*, *SM_b20752*, *cyoD*, *cyoC*, and *cyoB*, real-time quantitative PCR was performed with the following primers. *SMc02983*:
5'-GGCACAATCGTGCGTGTCCTTCAAC-3'
and 5'-GCCATTCGCCCATCTCAT-3';
SMc01578: 5'-GACTAGACTACGGTCCCAAC-3'
and 5'-TTATTACTCGCTCGTGATCTCATC-3';
SMc01656: 5'-GCCTTGTGTCTGAGGTTATCATC-3'
and 5'- CGTGGGAGGATGGCTCGAATG-3';
SMc02677: 5'- GCGTGCACAAGGGCCGCATGAG-3'
and 5'-CTCGGCGTCCTTGAGCACTCG-3';
SM_b20752: 5'-GGACGAGCGCCTGAACCACG-3'
and 5'-GCTCAGGAGCCATGCCTGTC-3';
cyoD: 5'-GCCTGGAGAGGCCGCATGAAG-3'
and 5'-GTCGCCGGTCCTTGAGACCTCG-3';
cyoB: 5'- CACTACGATACGGCTCCAAC-3'
and 5'-TTATTTACTCGCTCGGCCCTC-3';

cyoC: 5'-TGCAGGACGTTCGCGGAGCT- 3'
and 5'-GAGCGCAGCTCTGTCGG- 3'.
We used 16S rRNA as an internal reference gene to calculate normalized gene expression intensity using the Q-gene software (Muller et al. 2002).

The content of 17 amino acids was determined according to the method described by Sokolova et al. (2007) in an automatic amino acid analyzer (Hitachi 835–50 amino acid analyzer; Tokyo, Japan) with the measurement repeated three times for each sample. The *S. meliloti* respiratory complexes were measured using methods based on mitochondrial respiratory complex chain determination, as described by Vyatkina et al. (2004), and the enzyme activity was expressed as μmol min^{-1} mg^{-1} pro^{-1}. For this, 20 μl of the bacterial suspension was added to the PBS buffer, followed by the addition of 80 μM benzoquinone, 2 mM NaN_3, and 0.4 μM antimycin A (10 μl each). After mixing well, the mixture was incubated in a 28°C-water bath for 3 min, and then 10 μl of 200 μM NADH was added to start the reaction. Immediately after the reaction, a standard quartz cuvette was used to measure the OD value at 340 nm using a UV spectrophotometer. The CI activity was calculated using the standard curve.

Similarly, 50 μM 2,6-dichlorophenol indophenol, 2 mM NaN_3, 2 μg/ml rotenone, 2 μg/ml antimycin A, and 25 μM benzoquinone (10 μl each) were added to the buffer to which 20 μl of the bacterial suspension was added, and after mixing well, the mixture was incubated in a 28°C-water bath for 3 min, followed by the addition of 10 μl 20 μM sodium succinate to start the reaction. Immediately afterward, the OD value was measured with a standard quartz cuvette at 600 nm in a UV spectrophotometer. The CII activity was calculated from the standard curve.

As indicated above, 10 μl of 2 mM NaN_3 and 10 μl of 50 μM cytochrome c reductase were added sequentially to the buffer to which 20 μl of the bacterial suspension was added, and the mixture was incubated in a 28°C-water bath for 3 min, followed by the addition of 10 μl of 80 μM coenzyme Q to start the reaction. Immediately afterward, the OD value was measured with a standard quartz cuvette at 550 nm using a UV spectrophotometer. The CIII activity was determined from the standard curve.

Similarly, 10 μl of 0.025% *n*-dodecyl-*p*-D-maltoside was added to the buffer to which 20 μl of the bacterial suspension was added, and after mixing well, the mixture was incubated in a 28°C-water bath for 3 min, followed by the addition of 10 μl of 50 μM cytochrome c. The OD value was then measured immediately with a standard quartz cuvette at 550 nm using a UV spectrophotometer, and then the CIV activity was calculated from a standard curve. These measurements were repeated three times for each sample.

Results

Differentially expressed genes after hydrogen treatment. Analysis of the abundance of transcripts suggested that more than 99.58% of the sequenced data were meaningful. Relative to air-only control levels, 39 genes were downregulated and four genes were upregulated after hydrogen treatment for 72 h; the differential expression was defined as a fold change in expression level that was greater than 2. The fragments per kilobase of transcript per million fragments mapped (FPKM) values of differentially expressed genes before and after hydrogen treatment represented their expression levels, which were then used in the hierarchical clustering analysis. The clustering analysis resolved the three biological replicates into one class, indicating that the biological replicates were consistent and that the experimental results were reliable (Fig. 1). These genes are listed in Table I.

GO analysis. GO contains three parameters that describe the molecular function, cellular component,

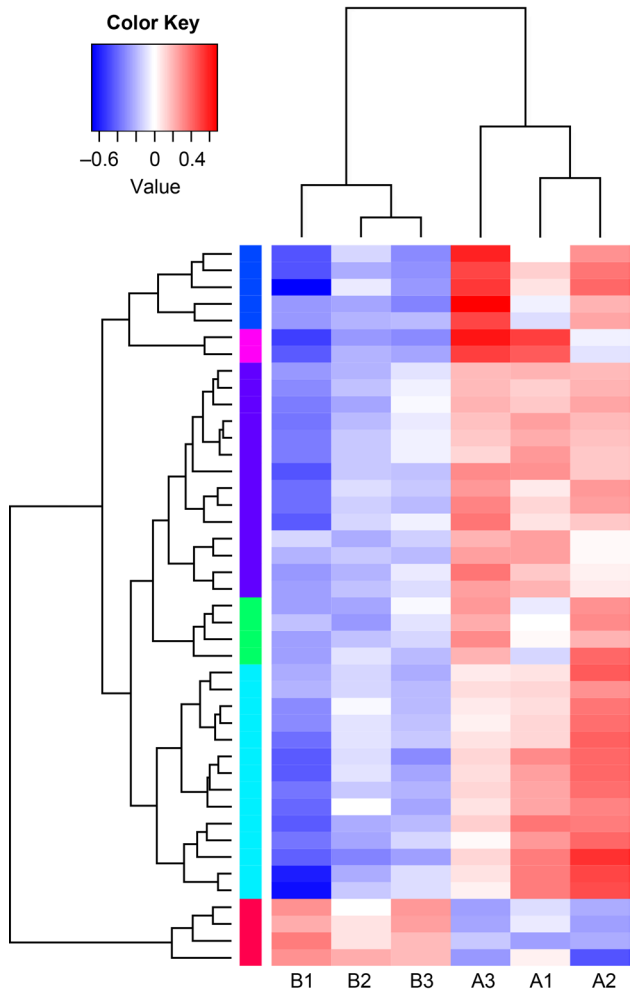

Fig. 1. Differential gene clustering. Red dots indicate downregulated genes and blue dots indicate upregulated genes in comparison with the control.

Table I
Differentially expressed genes – change with hydrogen treatment.

Gene ID	Gene name	Change with hydrogen treatment	Gene description
Gene1418	sugE	Down	Quaternary ammonium compound efflux SMR transporter SugE
Gene1984	msbB	Down	Lipid A biosynthesis (KDO)2-(lauroyl)-lipid IVA acyltransferase
Gene2119	SMc04350	Down	Multidrug efflux system transmembrane protein
Gene2120	SMc04351	Down	Transmembrane ATP-binding ABC transporter protein
Gene2494	mtlK	Down	Oxygen-independent coproporphyrinogen III oxidase
Gene2940	SMc02983	Down	Arginine decarboxylase
Gene3019	SMc03139	Ups	Hypothetical protein
Gene3089	SMc02519	Down	ABC transporter ATP-binding protein
Gene3090	SMc02518	Down	ABC transporter ATP-binding protein
Gene3090	SMc02518	Down	ABC transporter ATP-binding protein
Gene3091	SMc02517	Down	ABC transporter permease
Gene3471	SMa0081	Ups	ABC transporter permease
Gene361	iolB	Down	5-deoxy-glucuronate isomerase
Gene362	iolE	Down	Myo-inosose-2 dehydratase
Gene4065	SMa1163	Down	Cation transport P-type ATPase
Gene4073	SMa1176	Down	Hypothetical protein
Gene4075	nosR	Down	NosR regulatory protein for N2O reductase
Gene4076	nosZ	Down	Nitrous-oxide reductase
Gene4078	nosF	Down	NosF ATPase
Gene4079	nosY	Down	NosY permease
Gene4082	fhp	Down	Nitric oxide dioxygenase
Gene4092	fixI1	Down	ATPase
Gene4093	fixH	Down	Nitrogen fixation protein FixH
Gene4094	fixG	Down	FixG iron sulfur membrane protein
Gene4095	fixP1	Down	FixP1 di-heme cytochrome c
Gene4097	fixO1	Down	Cbb3-type cytochrome c oxidase subunit II
Gene4123	hemN	Down	Oxygen-independent coproporphyrinogen III oxidase
Gene4550	SMa2051	Down	Desaturase
Gene4551	SMa2053	Down	MocE-like protein
Gene5192	SM_b20487	Down	Sugar ABC transporter permease
Gene5193	SM_b20488	Down	Hypothetical protein
Gene5194	SM_b20489	Down	Carbohydrate kinase
Gene5727	groEL	Down	Chaperonin GroEL
Gene5728	groES5	Down	Molecular chaperone GroES
Gene6038	cyoB	Down	Cytochrome O ubiquinol oxidase subunit I
Gene6039	cyoC	Down	Cytochrome O ubiquinol oxidase subunit III
Gene6040	cyoD	Down	Cytochrome O ubiquinol oxidase CyoD
Gene6083	SM_b20654	Ups	Hypothetical protein
Gene6166	SM_b20753	Ups	Acyl-CoA dehydrogenase
Gene6288	agaL1	Down	Alpha-galactosidase (melibiase) protein
Gene811	groES	Down	Co-chaperone GroES (Cpn10) binds to Cpn60 in the presence of Mg-ATP and suppresses the ATPase activity of the latte
Gene968	betA	Down	Choline dehydrogenase
Gene969	betB	Down	Betaine aldehyde dehydrogenase
Gene970	betC	Down	Choline-sulfatase

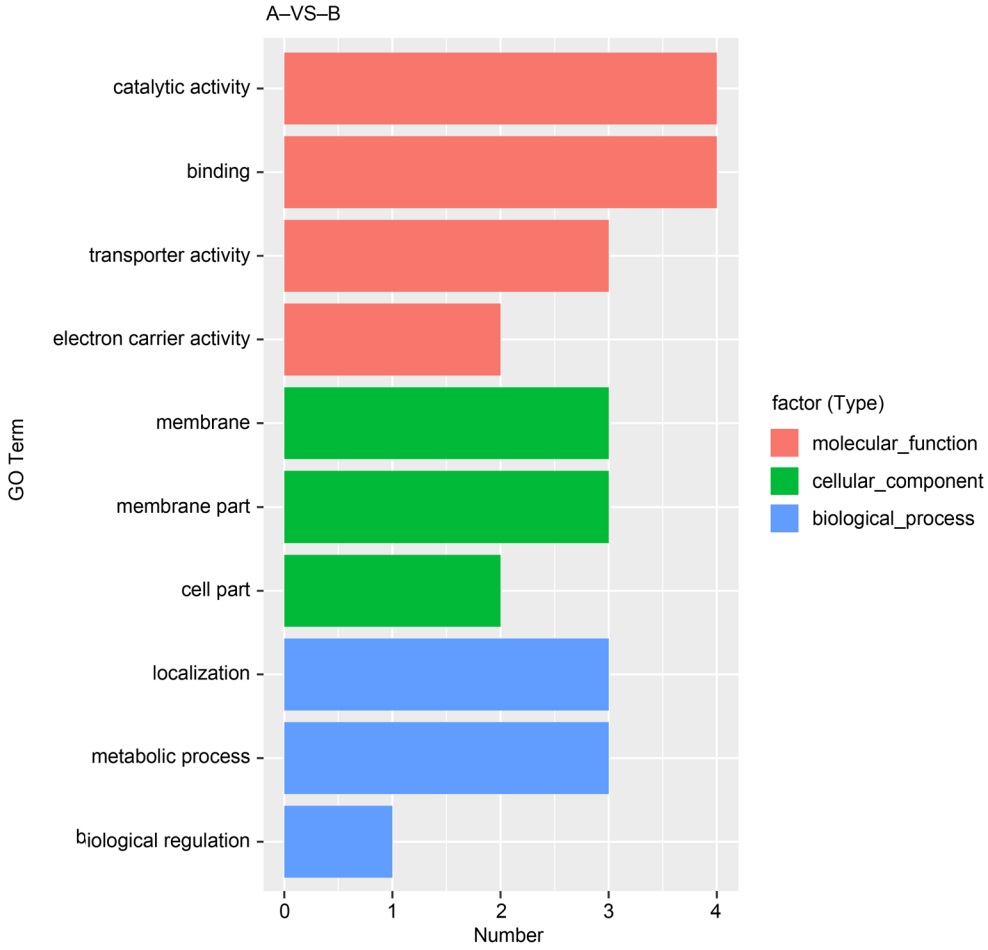

Fig. 2. Histogram of GO terms associated with differentially expressed genes; the GO term is on the ordinate; the number of differentially expressed genes associated with each term is on the abscissa.

and biological processes associated with the gene of interest. The differentially expressed genes under hydrogen treatment were classified into 10 main functions. In the molecular function category, 13 genes were associated with catalytic activity, binding, transporter activity, and electron carrier activity. In the cellular component category, eight genes were enriched; these were mainly involved in membrane and membrane components (Fig. 2). The genes associated with biological processes were primarily related to localization and metabolic process. Overall, the GO results indicated that hydrogen treatment primarily influences catalytic activity and binding of *S. meliloti* 1021. Eight of the differentially expressed genes (29% of the total) were associated with these two processes, suggesting that catalytic activity plays a crucial role in the response of *S. meliloti* to hydrogen.

KEGG pathway analysis and verification of related genes. A total of 3525 genes were assigned to 19 metabolic pathways from the KEGG database. The pathways were then restructured to categorize the differentially expressed genes into multiple classes. This revealed that 12 genes were involved in metabolic pathways; notably, the ABC transporter and oxidative phosphorylation pathways were modulated by hydrogen treatment. In addition, two of the downregulated genes were associated with two-component systems, inositol phosphate metabolism and glycine/serine/threonine metabolism. The detailed results are shown in Fig. 3.

During the KEGG pathway analysis, we noted that the arginine and proline metabolism pathway (ko00330) was downregulated in the hydrogen treatment group. To clarify this pathway's connection with hydrogen treatment, we checked if the pathway involves any hydrogenases. There are 3896 hydrogenases (IUBMB database, last accessed on January 2019). We shortlisted the hydrogenases (Table II) involved in the arginine and proline metabolism pathway to determine the effect of hydrogen treatment.

Hydrogen treatment caused a decrease in the expression of the gene encoding aminobutyraldehyde dehydrogenase (EC: 1.2.1.19), which is an important hydrogenase in the synthesis of 4-amino-butanoate and in β-alanine metabolism. Moreover, butanoate, alanine, glutamate, and ADC activities were also decreased under hydrogen treatment, which is the same

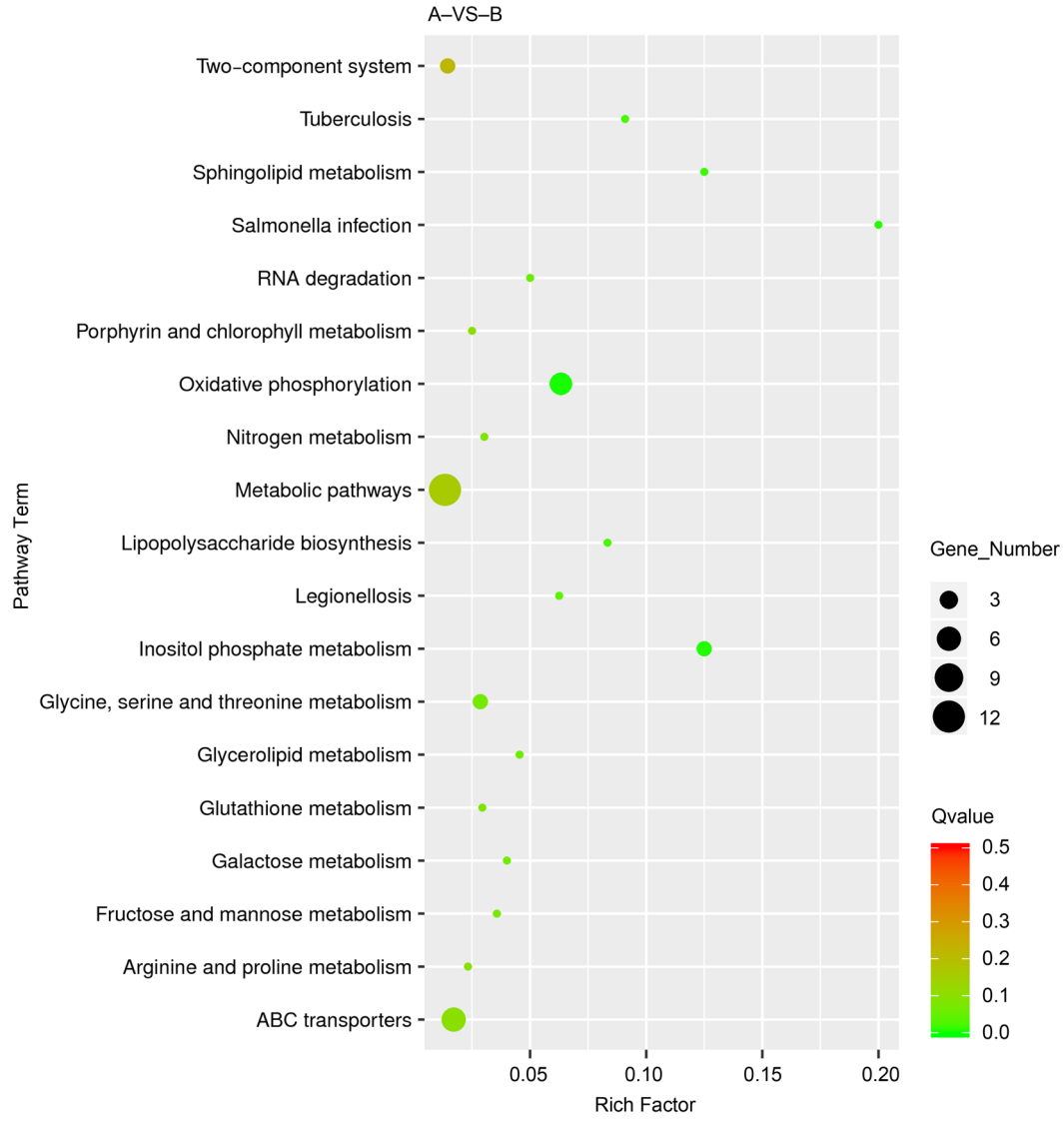

Fig. 3. Differential gene bubble map in the KEGG metabolic pathway.

outcome observed during the synthesis of β-alanine (ko00410).

The results of the amino acid analysis showed that the content of arginine, glycine, proline, serine, and threonine decreased after hydrogen treatment, and the content of arginine and proline exhibited the most significant decrease (Table III). After 72 h, the arginine content decreased by 0.47 mg g^{-1}, and the proline content decreased by 0.51 mg g^{-1}. The content of some other amino acids was elevated, but the increase was small.

Table II
Hydrogenases involved in arginine and proline metabolism.

EC number	Name
1.2.1.19	Aminobutyraldehyde dehydrogenase
1.2.1.3	Aldehyde dehydrogenase (NAD^+)
1.4.3.22	Diamine oxidase
1.2.1.71	Succinylglutamate-semialdehyde dehydrogenase
1.2.1.88	L-glutamate gamma-semialdehyde dehydrogenase
1.5.1.19	D-nopaline dehydrogenase
1.5.1.11	D-octopine dehydrogenase

Oxidative phosphorylation (ko00190) is an important aspect of metabolism and is closely related to nitrogen fixation (Allen and Arnon 1955). Hydrogen treatment increased the expression of cytochrome c oxidase (EC:1.9.3.1), inhibiting the H^+ consumption process in complex IV to reduce the intensity of oxidative phosphorylation.

Nitrogenase can capture large amounts of H^+ for nitrogen fixation, thereby reducing the consumption of H^+ in oxidative phosphorylation and providing energy for nitrogen fixation by nitrogenase (Millar et al. 1995).

Cytochrome O ubiquinol oxidase subunit I (*cyoB*), cytochrome O ubiquinol oxidase subunit III (*cyoC*), and cytochrome O ubiquinol oxidase CyoD (*cyoD*) are located on plasmid pSymB and participate in oxidative

Table III
The content of amino acids after hydrogen treatment.

Amino acid	Concentration (mg/g)			
	Control group	Test group		
		24 h	48 h	72 h
Alanine	0.32 ± 0.012	0.292 ± 0.03	0.342 ± 0.011	0.372 ± 0.05
Arginine	0.0842 ± 0.006	0.0682 ± 0.002	0.0622 ± 0008	0.0372 ± 0.004
Aspartic acid	1.822 ± 0.015	1.862 ± 0.3	1.882 ± 0.29	1.772 ± 0.24
Cysteine	0.182 ± 0.07	0.152 ± 0.04	0.222 ± 0.06	0.142 ± 0.03
Glutamic acid	2.12 ± 0.25	2.252 ± 0.16	2.242 ± 0.19	2.22 ± 0.11
Glycine	0.0772 ± 0.004	0.0742 ± 0.006	0.0712 ± 0.003	0.0682 ± 0.009
Histidine	0.162 ± 0.07	0.182 ± 0.09	0.172 ± 0.05	0.152 ± 0.02
Isoleucine	0.72 ± 0.037	0.682 ± 0.02	0.772 ± 0.03	0.732 ± 0.08
Leucine	0.252 ± 0.022	0.222 ± 0.03	0.262 ± 0.04	0.292 ± 0.05
Lysine	3.62 ± 0.17	3.42 ± 0.11	3.32 ± 0.2	3.72 ± 0.19
Methionine	0.092 ± 0.003	0.062 ± 0.001	0.092 ± 0.004	0.0122 ± 0.002
Phenylalanine	1.52 ± 0.08	1.72 ± 0.05	1.622 ± 0.07	1.582 ± 0.03
Proline	0.0732 ± 0.002	0.0642 ± 0.008	0.0262 ± 0.002	0.0222 ± 0.004
Serine	0.0652 ± 0.007	0.0612 ± 0.002	0.062 ± 0.008	0.0552 ± 0.007
Threonine	0.0782 ± 0.005	0.0772 ± 0.005	0.0542 ± 0.007	0.0582 ± 0.003
Tyrosine	None	None	None	None
Valine	0.062 ± 0.003	0.0622 ± 0.007	0.0642 ± 0.004	0.0672 ± 0.008

phosphorylation. *SMc02983* encodes arginine decarboxylase, *SMc01656* encodes gamma-aminobutyraldehyde dehydrogenase, *SM_b20752* encodes 3-hydroxyisobutyryl-CoA hydrolase, *SMc01578* encodes aspartate aminotransferase, and *SMc02677* (*proC*) encodes pyrroline-5-carboxylate reductase; these genes are involved in arginine and proline metabolism. The transcription levels of *SMc02983*, *SMc01656, SMc01578, SMc02677, SM_b20752*, *cyoB*, *cyoC*, and *cyoD,* before and after hydrogen treatment, were measured by real-time quantitative PCR (Fig. 4). *SMc02983* and *cyoB* showed a difference after 24 h, and the differential expression levels were 0.72 and 0.59, respectively; this difference reached the maximum (1.52 and 1.29) after 72 h. However, the difference for *cyoC* was maximal (1.06) at 48 h, after which it decreased. The expression of *cyoD* gene showed the least difference after 24 h, but it increased and showed a maximum difference of 1.27 after 72 h. The genes *SMc02677* and *SM_b20752* were upregulated, and the fold difference was the highest at 48 h (0.55) and 72 h (0.85), respectively. The data are consistent with the RNA-seq data, indicating

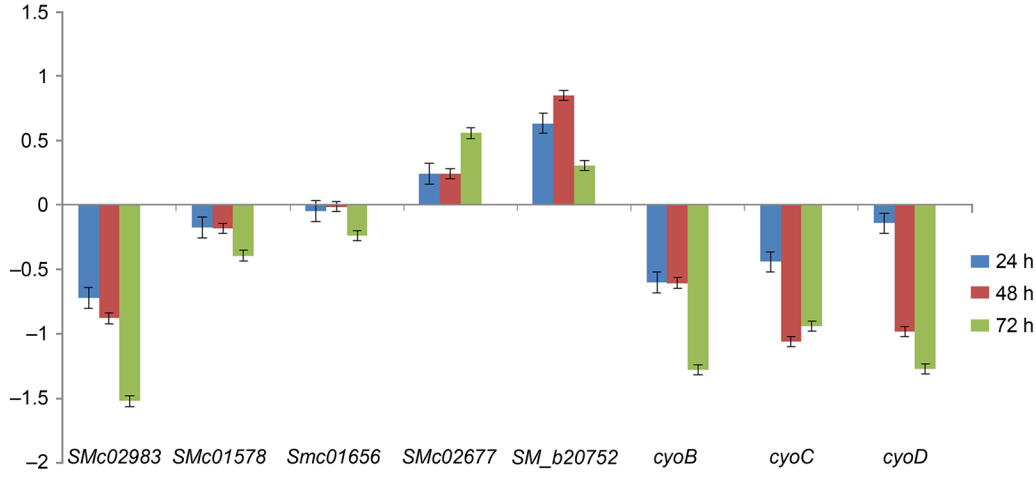

Fig. 4. Fold change in the expression levels of SMc02983, SMc01578, SMc01656, SMc02677, SM_b20752, cyoD, cyoB, and cyoC after the hydrogen treatment as determined by real-time quantitative PCR.

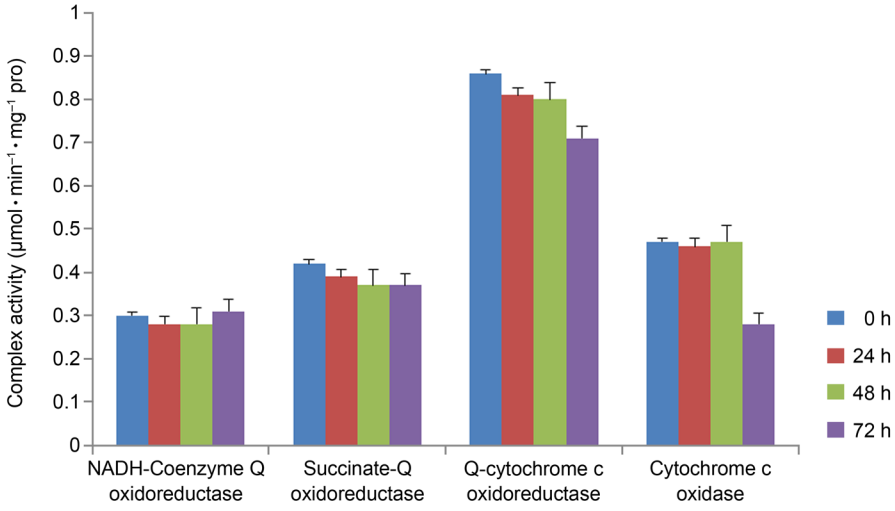

Fig. 5. The oxidative phosphorylation complex activity map. Each experiment was performed three times.

that the expression of the four genes was significantly downregulated. Among these, *SMc02983* had the highest reduction in expression.

The results of oxidative phosphorylation complex activity showed that hydrogen treatment reduced the activity of complex IV most significantly. There may also be other mechanisms underlying the role of CIV activity in reducing complex II activity by regulating the electron transfer between CIII and CIV (Fig. 5).

Discussion

S. meliloti can live as a soil saprophyte and engage in nitrogen-fixing symbiosis with plant roots (Barnett et al. 2012). A large amount of hydrogen is produced during nitrogen fixation in symbioses (Osborne et al. 2010). *S. meliloti* 1021 is an important N_2-fixing bacterium in the root nodule of legumes (Capela et al. 2001). It is a model strain for studying Rhizobium and has further research value. At present, there are many studies on drought and heavy metals, and few studies have focused on how hydrogen affects Rhizobium (Elboutahiri et al. 2010). In this study, the effect of hydrogen on Rhizobium was analyzed using RNA-Seq technology. The response to hydrogen treatment was visualized through up- and down-regulated genes. Hydrogen primarily affected amino acid metabolism. Hydrogen-metabolizing organisms use [NiFe]-hydrogenase to catalyze hydrogen oxidation and the NAD^+-reducing soluble [NiFe]-hydrogenase (SH) couples reduction of NAD^+ to the oxidation of hydrogen (Vinson 2017). Hydrogenases catalyze the oxidation of hydrogen into protons and electrons, to use H_2 as an energy source or for the production of hydrogen through proton reduction (Albareda et al. 2012). This is consistent with the findings of several studies that indicated amino acid metabolism to be a major feature of the *S. meliloti* chromosome (Capela et al. 2001). Consistent with these reports, we found that aminobutyraldehyde dehydrogenase is primarily involved in arginine, proline, and β-alanine metabolism, and its expression is downregulated. The determination of amino acid content also revealed a decrease in the content of proline and arginine. A proline catabolic mutant had a negligible impact on nitrogenase activity as evaluated through acetylene reduction (Chien et al. 1991). However, *S. meliloti* exhibited positive chemotactic responses to all proteinogenic amino acids, except aspartate, citrulline, cysteine, gamma-aminobutyric acid, and ornithine (Webb et al. 2017). Hydrogen treatment provided microaerobic conditions to *S. meliloti* 1021. Expression of genes involved in nitrogen fixation and the associated respiration is governed by two intermediate regulators, NifA and FixK, respectively, which are controlled by a two-component regulatory system FixLJ in response to low-oxygen conditions. FixJ controls 74% of the genes induced in microaerobiosis (2% oxygen) (Bobik et al. 2006). According to Defez's research, under microaerobic conditions, the overexpression of IAA in free-living *S. meliloti* cells induced many of the transcriptional changes that normally occur in nitrogen-fixing root nodules (Defez et al. 2016). Therefore, hydrogen treatment, in this study, restricted the two pathways containing hydrogenase, but provided a micro-oxygen environment for *S. meliloti*. Further, the fixN gene and cyoB and cyoD genes were downregulated. Real-time quantitative PCR results showed that some genes have no reaction time for hydrogen; nonetheless, the genes involved in the metabolism of arginine and proline were the most different, indicating that amino acid synthesis is an important biological process of *S. meliloti* 1021. The expression of *SMc02677, SM_b20752,* and other genes partially metabolized by arginine and pro-

line was upregulated. These genes were not screened for the transcriptome differential genes. Therefore, after reducing the screening of multiple differential genes, the expression of genes related to nitrogen fixation and amino acid synthesis was upregulated.

The differential genes involved in the experiments were annotated in several aspects. Based on previous studies, we focused on hydrogenase pathways. These genes were verified by real-time quantitative PCR and were found to be consistent with RNA-Seq findings. Therefore, the research is somewhat reliable. Taken together, hydrogen affects *S. meliloti* 1021 by affecting amino acid synthesis and oxidative phosphorylation processes. It may be associated either with the competition for carbon compounds imported into the nodules between the energy production and nitrogen assimilation processes or with the competition for redox potentials between the oxidative phosphorylation and nitrogen fixation processes (Provorov et al. 2013). We speculate that hydrogen is a beneficial factor for the symbiotic system of *S. meliloti* 1021. Previous studies have shown that the release of hydrogen to the soil has a beneficial effect and that the development of PGPR as the seed inoculants is an important step toward sustainable agriculture (Golding 2009). As an important type of PGPR, *S. meliloti* 1021 has potential development significance for the symbiosis between legumes and rhizobia. This study explores these beneficial effects of the *S. meliloti* 1021 metabolic processes.

Conclusion

We determined the transcriptomic changes in *S. meliloti* 1021 under the hydrogen treatment. Overall, the results demonstrate that hydrogen alters the expression of genes related to aminobutyraldehyde dehydrogenase and cytochrome c oxidase, which in turn affect metabolic pathways, especially those involved in amino acid metabolism and oxidative phosphorylation. These results may provide a theoretical basis for more effective agricultural exploitation of *S. meliloti* 1021.

Funding

This work was supported by the National Natural Science Foundation of China (41571243).

Acknowledgments

We thank the GENEWIZ Company for their help in RNA--sequencing.

Conflict of interest

The authors do not report any financial or personal connections with other persons or organizations, which might negatively affect the contents of this publication and/or claim authorship rights to this publication.

Literature

Albareda M, Manyani H, Imperial J, Brito B, Ruiz-Argüeso T, Böck A, Palacios JM. Dual role of HupF in the biosynthesis of [NiFe] hydrogenase in *Rhizobium leguminosarum*. BMC Microbiol. 2012;12(1):256–256. https://doi.org/10.1186/1471-2180-12-256

Allen MB, Arnon DI. Studies on nitrogen-fixing blue-green algae. I. Growth and nitrogen fixation by *Anabaena cylindrica* Lemm. Plant Physiol. 1955 Jul 01;30(4):366–372.
, https://doi.org/10.1104/pp.30.4.366

Barnett MJ, Bittner AN, Toman CJ, Oke V, Long SR. Dual RpoH sigma factors and transcriptional plasticity in a symbiotic bacterium. J Bacteriol. 2012 Sep 15;194(18):4983–4994.
https://doi.org/10.1128/JB.00449-12

Barnett MJ, Fisher RF, Jones T, Komp C, Abola AP, Barloy-Hubler F, Bowser L, Capela D, Galibert F, Gouzy J, et al. Nucleotide sequence and predicted functions of the entire *Sinorhizobium meliloti* pSymA megaplasmid. Proc Natl Acad Sci USA. 2001 Aug 14;98(17):9883–9888.
https://doi.org/10.1073/pnas.161294798

Bobik C, Meilhoc E, Batut J. FixJ: a major regulator of the oxygen limitation response and late symbiotic functions of *Sinorhizobium meliloti*. J Bacteriol. 2006 Jul 01;188(13):4890–4902.
https://doi.org/10.1128/JB.00251-06

Capela D, Barloy-Hubler F, Gouzy J, Bothe G, Ampe F, Batut J, Boistard P, Becker A, Boutry M, Cadieu E, et al. Analysis of the chromosome sequence of the legume symbiont *Sinorhizobium meliloti* strain 1021. Proc Natl Acad Sci USA. 2001 Aug 14;98(17):9877–9882. https://doi.org/10.1073/pnas.161294398

Chien CT, Rupp R, Beck S, Orser CS. Proline auxotrophic and catabolic mutants of *Rhizobium leguminosarum* biovar *viciae* strain C1204b are unaffected in nitrogen fixation. FEMS Microbiol Lett. 1991 Jan;77(2–3):299–302.
https://doi.org/10.1111/j.1574-6968.1991.tb04365.x

Cunningham SD, Kapulnik Y, Phillips DA. Distribution of hydrogen-metabolizing bacteria in Alfalfa field soil. Appl Environ Microbiol. 1986;52(5):1091–1095.
https://doi.org/10.1128/AEM.52.5.1091-1095.1986

Defez R, Esposito R, Angelini C, Bianco C. Overproduction of indole-3-acetic acid in free-living Rhizobia induces transcriptional changes resembling those occurring in nodule bacteroids. Mol Plant Microbe Interact. 2016 Jun;29(6):484–495.
https://doi.org/10.1094/MPMI-01-16-0010-R

Dong Z, Wu L, Kettlewell B, Caldwell CD, Layzell DB. Hydrogen fertilization of soils – is this a benefit of legumes in rotation? Plant Cell Environ. 2003 Nov;26(11):1875–1879.
https://doi.org/10.1046/j.1365-3040.2003.01103.x

Elboutahiri N, Thami-Alami I, Udupa SM. Phenotypic and genetic diversity in *Sinorhizobium meliloti* and *S. medicae* from drought and salt affected regions of Morocco. BMC Microbiol. 2010;10(1):15–0. https://doi.org/10.1186/1471-2180-10-15

Galibert F, Finan TM, Long SR, Pühler A, Abola P, Ampe F, Barloy-Hubler F, Barnett MJ, Becker A, Boistard P, et al. The composite genome of the legume symbiont *Sinorhizobium meliloti*. Science. 2001 Jul 27;293(5530):668–672.
https://doi.org/10.1126/science.1060966

Golding AL. H_2-oxidizing, plant growth promoting rhizobacteria as seed inoculants for barley. Halifax (Canada): Saint Mary's University; 2009.

Hesterman OB, Sheaffer CC, Barnes DK, Lueschen WE, Ford JH. Alfalfa dry matter and nitrogen production and fertilizer nitrogen response in leguminous-corn rotation. Agron J. 1986 Jan;78(1):19–23.
https://doi.org/10.2134/agronj1986.00021962007800010005x

Kanehisa M, Goto S. KEGG: Kyoto Encyclopedia of Genes and Genomes. Nucleic Acids Res. 2000;28:27–30.

Kärst U, Suetin S, Friedrich CG. Purification and properties of a protein linked to the soluble hydrogenase of hydrogen-oxidizing bacteria. J Bacteriol. 1987;169(5):2079–2085. https://doi.org/10.1128/JB.169.5.2079-2085.1987

La Favre JS, Focht DD. Conservation in soil of H_2 liberated from N_2 fixation by Hup-nodules. Appl Environ Microbiol. 1983;46(2): 304–311. https://doi.org/10.1128/AEM.46.2.304-311.1983

Langmead B, Salzberg SL. Fast gapped-read alignment with Bowtie 2. Nat Methods. 2012 Apr;9(4):357–359. https://doi.org/10.1038/nmeth.1923

Li J, Han S, Ding X, He T, Dai J, Yang S, Gai J. Comparative transcriptome analysis between the cytoplasmic male sterile line NJCMS1A and its maintainer NJCMS1B in soybean (*Glycine max* (L.) Merr.). PLoS One. 2015 May 18;10(5):e0126771. https://doi.org/10.1371/journal.pone.0126771

López M, Carbonero V, Cabrera E, Ruiz-Argüeso T. Effects of host on the expression of the H_2-uptake hydrogenase of Rhizobium in legume nodules. Plant Sci Lett. 1983 Apr;29(2–3):191–199. https://doi.org/10.1016/0304-4211(83)90143-8

McLearn N, Dong Z. Microbial nature of the hydrogen-oxidizing agent in hydrogen-treated soil. Biol Fertil Soils. 2002 Jul 1;35(6): 465–469. https://doi.org/10.1007/s00374-002-0495-z

Millar AH, Day DA, Bergersen FJ. Microaerobic respiration and oxidative phosphorylation by soybean nodule mitochondria: implications for nitrogen fixation. Plant Cell Environ. 1995 Jul; 18(7): 715–726. https://doi.org/10.1111/j.1365-3040.1995.tb00574.x

Muller PY, Janovjak H, Miserez AR, Dobbie Z. Processing of gene expression data generated by quantitative real-time RT-PCR. Biotechniques. 2002 Jun;32(6):1372–1374, 1376, 1378–1379.

Osborne CA, Peoples MB, Janssen PH. Detection of a reproducible, single-member shift in soil bacterial communities exposed to low levels of hydrogen. Appl Environ Microbiol. 2010 Mar 01;76(5):1471–1479. https://doi.org/10.1128/AEM.02072-09

Parry R, Asgari S. *Aedes anphevirus*: an insect-specific virus distributed worldwide in *Aedes aegypti* mosquitoes that has complex interplays with *Wolbachia* and dengue virus infection in cells. J Virol. 2018 Jun 27;92(17):e00224-18. https://doi.org/10.1128/JVI.00224-18

Provorov NA, Chuklina E, Vorob'ev NI, Onishchuk OP, Simarov BV. [Factor analysis of interactions between alfalfa nodule bacteria (*Sinorhizobium meliloti*) genes that regulate symbiotic nitrogen fixation] (in Russian). Genetika. 2013 Apr;49(4):448–453. https://doi.org/10.7868/s0016675813030156

Sokolova MG, Akimova GP, Nechaeva LV, Permyakov AV, Sobenin AM. The effect of inoculation with Rhizobium leguminosarum on the contents of cytoplasmic protein and free amino acids in the roots of pea seedlings. Appl Biochem Microbiol. 2007 May;43(3):268–273. https://doi.org/10.1134/S0003683807030064

Spaink HP. Root nodulation and infection factors produced by rhizobial bacteria. Annu Rev Microbiol. 2000 Oct;54(1):257–288. https://doi.org/10.1146/annurev.micro.54.1.257

Taylor AB, Smith BS, Kitada S, Kojima K, Miyaura H, Otwinowski Z, Ito A, Deisenhofer J. Crystal structures of mitochondrial processing peptidase reveal the mode for specific cleavage of import signal sequences. Structure. 2001 Jul;9(7):615–625. https://doi.org/10.1016/S0969-2126(01)00621-9

Vinson V. How a hydrogenase protects its active site. Science. 2017 Sep 01;357(6354);882–884. https://doi.org/10.1126/science.357.6354.882-n

Vyatkina G, Bhatia V, Gerstner A, Papaconstantinou J, Garg N. Impaired mitochondrial respiratory chain and bioenergetics during chagasic cardiomyopathy development. Biochimica et Biophysica Acta (BBA) – Molecular Basis of Disease. 2004 Jun;1689(2): 162–173. https://doi.org/10.1016/j.bbadis.2004.03.005

Wang F, Wang C, Sun Y, Wang N, Li X, Dong Y, Yao N, Liu X, Chen H, Chen X, et al. Overexpression of vacuolar proton pump ATPase (V-H+–ATPase) subunits B, C and H confers tolerance to salt and saline-alkali stresses in transgenic alfalfa (*Medicago sativa* L.). J Integr Agric. 2016 Oct;15(10):2279–2289. https://doi.org/10.1016/S2095-3119(16)61399-0

Webb BA, Compton KK, Del Campo JSM, Taylor D, Sobrado P, Scharf BE. *Sinorhizobium meliloti* chemotaxis to multiple amino acids is mediated by the chemoreceptor McpU. Mol Plant Microbe Interact. 2017 Oct;30(10):770–777. https://doi.org/10.1094/MPMI-04-17-0096-R